

opposing air bearings configuration, the bearing pads are often installed in some enclosed carriage. Direct measurement of the actual air gap is difficult. To address this practical limitation, most tend to take the lift measured from the top of the bearing mounting mechanism in the carriage as an acceptable estimate of the air gap height, assuming the mounting mechanism as a perfectly rigid connection. The lack of understanding of the air bearing system, and an accurate description of the stiffness model of individual air bearing setup hinder the development of a robust guideway model which are essential in the design of precision mechatronic system. In this work, an aerostatic guideway identical to the one shown in Figure 1 was used. The subsequent sections demonstrate the ease of predicting accurate modal frequencies of the above guideway carriage when the proposed air gap estimation and effective stiffness of the bearing system are employed.

2 Air Gap Estimation and the Effective Stiffness of an Air Bearing System

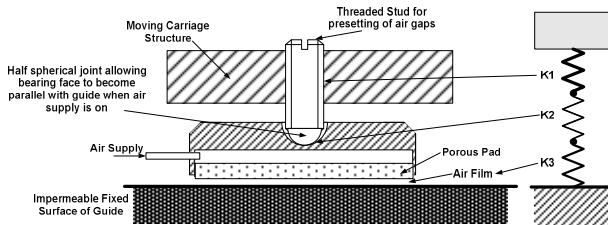


Figure 2: Air Bearing Mounting

A typical air bearing pad is made up of several interfaces/connections which contribute to the overall stiffness of a single bearing system. We can understand this as a number of linear or nonlinear springs connected in series, as illustrated in Figure 2. Besides the air film stiffness, K_3 , there are two other interfaces that may contribute to the overall stiffness of the air bearing mounting: the threaded stud in the structure, labelled as stiffness K_1 in Figure 2; and the spherical joint, labelled as K_2 . Under proper preloading, K_1 is found to be much stiffer than K_2 and K_3 , usually in the magnitude of tens of $\text{KN}/\mu\text{m}$ [1]. Therefore, K_1 is assumed to be a rigid connection in the system. The modelling of aerostatic air film stiffness has been discussed extensively [4-6]. In our work, the stiffness of the air film is computed using the 1D flow method proposed by [5]. The investigation of the spherical joint interface

stiffness was carried out in [6]. When specific air pressure is supplied to all the air bearings, the force exerted by the opposing air bearings creates an air gap displacement and a Hertzian contact deformation in the spherical joint. These two ‘internal’ displacements result in an effective (external) lift at the top of the bearing mounting mechanism. The ‘external’ displacement can be easily measured and used to estimate the two ‘internal’ displacements, which in terms give the nominal stiffnesses of the air film and spherical joint. Both the air film and spherical joint stiffnesses are non-linear and are obtained either numerically or experimentally [1]. The most effective way is to estimate the above values graphically. Figure 3 shows how these values can be obtained graphically for an opposing air bearings setup where the external displacement is measured at $9\ \mu\text{m}$. The stiffness and displacement curves of the spherical joint are offset to $9\ \mu\text{m}$ to reflect the external displacement. The internal displacements occur at the equilibrium point of the force interact between the air film and the spherical joint, i.e. the intersection of the two load vs displacement curves, as illustrated in Figure 3.

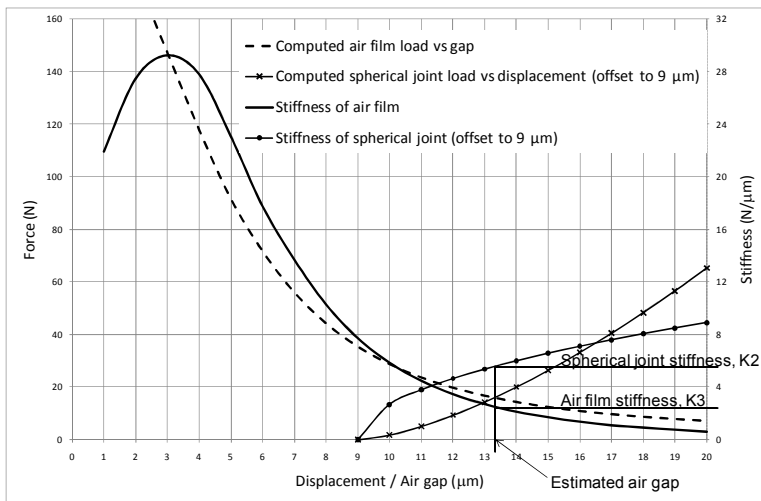


Figure 3: Estimation of air gap and spherical joint displacements/stiffnesses

3 Modal Frequencies Computation of Aerostatic Guideway

The structural dynamic behaviour of the guideway system is not considered in this investigation. Hence, the first five (finite frequency) modes of the guideway will correspond to the five constrained DOFs of the carriage. X axis is unconstrained.

These modes are mainly influenced by the stiffness of the air bearings. Hence, the dynamic behaviour of the carriage can be simplified into a model as illustrated by Figure 4.

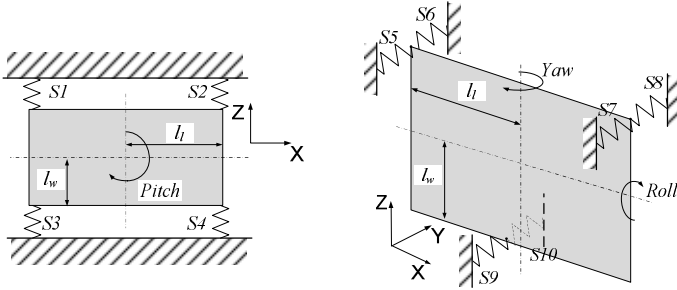


Figure 4: Simplified model of air bearing carriage

Based on the simplified model, the stiffness matrix $[K]$ of the carriage, in terms of translation in Y and Z and rotations in roll, pitch and yaw, takes the form of a 5×5 diagonal matrix,

$$[K] = \text{diag}(6K_e, 4K_e, 6K_e l_w^2, 4K_e l_t^2, 4K_e l_t^2) \quad (1)$$

where K_e is the effective stiffness of each air bearing represented by the springs, S1 to S10 in Figure 4, and are assumed to possess the same stiffness. The effective stiffness K_e is simply the combined value of $K2$ and $K3$ in series. The modal frequencies, $\bar{\omega}_r$, of the carriage can be expressed as

$$\begin{bmatrix} -2 \\ \bar{\omega}_r \end{bmatrix} = \text{diag} \left(\frac{6K_e}{m_c}, \frac{4K_e}{m_c}, \frac{6K_e l_w^2}{I_{xx}}, \frac{4K_e l_t^2}{I_{yy}}, \frac{4K_e l_t^2}{I_{zz}} \right) \quad (2)$$

where m_c is the mass of the carriage, and I_{xx} , I_{yy} , and I_{zz} are the moment of inertia about X, Y and Z axes, respectively.

4 Results and Conclusion

The computed frequencies (based on the estimated stiffnesses, $K2$ and $K3$, and Equation 2) are verified using Finite Element Modal Analysis (FEMA) of the aerostatic guideway to ensure that the model illustrated in Figure 4 is not oversimplified. The analytically computed and FEMA results achieve more than 95% agreement. Experimental modal tests are performed on the aerostatic carriage. The experimental modal results correspond closely to the above computed

frequencies, with approximately 77% to 94% agreements. The consistency of the proposed approach was verified by varying the supply pressure (to create different air bearing stiffness), and the results were similar.

This study demonstrated the significance of air bearing mounting mechanisms to the static and dynamic behaviour of aerostatic guideways, which are often neglected in the modelling process. The proposed approach reduces the air bearing model uncertainties for inaccessible air bearing mounting setup. The model develop for air gap height through the joint and air film stiffnesses increases the robustness and accuracy of aerostatic guideway static and dynamic model.

References:

- [1] C.W. Lim, “Dynamic Analysis of Aerostatic Guideway and FEA Model Development”, EngD Thesis, Cranfield University, 2010.
- [2] R. Cortesi, “An easy to manufacture non-contact precision linear motion system and its applications”, MSc thesis, Massachusetts Institute of Technology, 2006.
- [3] B. O’Connor, “Modelling and analysis of porous graphite air bearings”, MSc Thesis, The Pennsylvania State University, 2000.
- [4] Y. B. P. Kwan and J. Corbett, “Porous aerostatic bearings-an updated review”, *Wear*, vol. 222, no. 2, pp. 69–73, 1998.
- [5] J. S. Plante, J. Vogan, T. El-Aguizy, and A. H. Slocum, "A design model for circular porous air bearings using the 1D generalized flow method," *Precision Engineering*, vol. 29, no. 3, pp. 336-346, July2005.
- [6] C.W. Lim, P. Shore, P. Morantz, W. Lin and W. J. Wills-Moren, “Dynamic Modelling and Testing of Air Bearing Interfaces”, *Euspen Conference Proceeding*, Vol. 1, pp. 184-188, May 2008.